Phase transitions, aggregation and crystallization in mixed suspensions of colloidal spheres and rods

G. A. Vliegenthart,[a] A. van Blaaderen[a,b] and H. N. W. Lekkerkerker[a]

[a] *Van't Hoff Laboratory for Physical and Colloid Chemistry, Debye Institute, Utrecht University, Padualaan 8, 3584 CH Utrecht, The Netherlands*
[b] *FOM Institute for Atomic and Molecular Physics, PB 41883, 1009 DB, Amsterdam, The Netherlands*

Received 11th February 1999

We have studied the coupling of aggregation and crystallization in a mixture of colloidal spheres and colloidal rods. Taking advantage of specially prepared fluorescent silica spheres we are able to investigate this process at the particle level by fluorescense confocal microscopy. We find that above a limiting concentration of rods in the mixture, the spheres rapidly assemble to form compact aggregates which subsequently crystallize.

I Introduction

In 1954 Asakura and Oosawa[1] showed that the addition of non-adsorbing polymer to a dispersion of colloidal particles will lead to an effective attractive interaction. This result was independently recovered and further elaborated by Vrij[2] in 1976. The attractive interaction, which is called depletion interaction, is the origin of the rich phase behavior displayed by colloid–polymer mixtures.

The depletion interaction can be explained in terms of purely repulsive interactions between the polymers and the colloidal particles. Each colloidal particle is surrounded by a shell with a thickness of the order of the radius of gyration of a polymer molecule through which the center of the polymer cannot penetrate. This excluded region is called the depletion zone. When two colloidal particles approach each other such that their respective depletion zones start to overlap, the available volume for the polymer increases. This extra volume in turn causes the total entropy to increase and the free energy to decrease. In other words, the colloidal particles experience an effective attraction.

In the last two decades significant progress has been made in understanding the phase behavior of colloid–polymer mixtures. This progress has been achieved by extensive experimental work on a variety of (model) systems,[3–8] the development of theoretical concepts and tools[9,10] and computer simulations.[11] For various systems, the phase diagrams have now been determined experimentally, showing colloidal gas–liquid, colloidal gas–solid and colloidal fluid–solid phase equilibria. At the same time, quenches deeper in the two phase region of the phase diagram show a transition of equilibrium states to non-equilibrium states.[12,13] This is illustrative for the rich phase behavior displayed by colloid–polymer mixtures.

The depletion interaction mechanism is not limited to colloid–polymer mixtures. Using the same entropy argument as for colloid–polymer mixtures, mixtures of different size and/or shape are expected to exhibit similar phase behavior. In the case of binary mixtures of large and small

colloidal hard spheres, the depletion potential is in lowest order in the density given by,[1,14]

$$W(h) = -3k_B T\phi \frac{R}{\sigma}\left(1 - \frac{h}{\sigma}\right)^2 \quad (1)$$

Here, $k_B T$ is the thermal energy, ϕ is the volume fraction of the small spheres, R the radius of the large spheres, σ the diameter of the small spheres, and h the distance between the surfaces of the two large spheres. To obtain a rough estimate of the volume fraction needed to induce phase separation, we assume that such a phase transition requires an attraction between the particles of the order of a few, say, $-3\ k_B T$. Eqn. (1) then implies that for a size ratio $2R/\sigma = 10$ the depletion interaction will cause phase separation when the volume fraction of small spheres is about 20%. Indeed, in mixtures of large and small spheres, phase transitions have been predicted,[15,16] observed experimentally[17–20] and by simulations[21–23] around this volume fraction of small spheres.

An even more interesting colloidal mixture from a depletion interaction point of view is that of colloidal spheres and colloidal rods. This was already recognized by Asakura and Oosawa who mentioned rod-like macromolecules as depletion agents in their 1958 paper.[24] Auvray[25] derived an expression for the depletion interaction potential due to thin rods in the Derjaguin approximation. More recently Mao *et al.*[26] calculated the depletion interaction of rods of length L and diameter D up to third order in the density of the rods. In the limit that the length L of the rod-like particles is much smaller than the radius R of the colloidal spheres, the depletion potential to the lowest order in density is given by,

$$W(h) = -\tfrac{2}{3}k_B T\phi \frac{L}{D}\frac{R}{D}\left(1 - \frac{h}{L}\right)^3 \quad (2)$$

where ϕ is now the volume fraction of the rods. From eqn. (2) we estimate that for the case $R/L = 2$ and $L/D = 20$ a minimum value of the depletion interaction of $-3k_B T$ is obtained when the volume fraction ϕ of rods is only about 0.5%. Without the Derjaguin approximation, a calculation to first order in the density gives a slightly higher volume fraction of rods for which demixing is expected to occur.[27] Clearly, rod-like particles are very efficient depletion agents; very low concentrations of rods are predicted to lead to phase separation. This also follows from detailed numerical simulations on mixtures of spheres and infinitely thin rods.[28]

The theoretical arguments given above result in a first estimate of the concentrations of rods needed to induce a phase transition. Here we present a theory that allows for the calculation of the phase diagram of a rod–sphere mixture which can be compared with experimental data. Recently we have observed for the first time phase separation in mixed suspensions of rods and spheres.[29] Colloidal crystals of silica spheres were observed upon addition of a small amount of boehmite rods. In this paper we report on the crystallization mechanism in those mixtures. Taking advantage of specially prepared fluorescent silica spheres of about 740 nm (diameter), the crystallization process was followed at particle level in real time and real space by confocal microscopy.[30] The phenomena observed in our colloidal mixed colloidal system, suggest a two-stage crystallization process. Rapid aggregation of the colloidal spheres is followed by slow rearrangement into crystals.

II Theory

The phase diagram of a mixture of colloidal spheres of radius R (component 1) and of hard colloidal rods with length L and diameter D (component 2) can be calculated using the osmotic equilibrium approach.[10] Consider the osmotic equilibrium system illustrated in Fig. 1. A reservoir with rods at chemical potential μ_2 is in osmotic equilibrium with a system of volume V containing N_1 large spheres. The thermodynamic potential $\Omega(N_1, V, T, \mu_2)$ for the system can be written as,

$$\begin{aligned}\Omega &= F + \int_{-\infty}^{\mu_2}\left(\frac{\partial\Omega}{\partial\mu_2}\right)_{N_1, V, T} \mathrm{d}\mu_2 \\ &= F - \int_{-\infty}^{\mu_2} N_2\, \mathrm{d}\mu_2 \end{aligned} \quad (3)$$

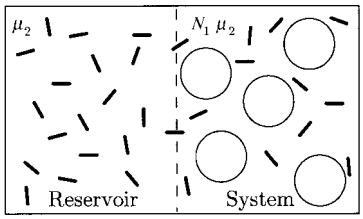

Fig. 1 Osmotic equilibrium model. Two compartments are in osmotic equilibrium through a permeable membrane. The left compartment (reservoir) contains the rods at chemical potential μ_2. The right compartment (system) contains N_1 spheres in a volume V at temperature T and $\langle N_2 \rangle$ rods at chemical potential μ_2.

Where $F(N_1, V, T)$ is the Helmholtz free energy for the pure sphere system. In the limit where the density of the rods in the reservoir $\rho_2^{\mathrm{R}} \to 0$, the number of rods in the system N_2 is given by,

$$N_2 = \rho_2^{\mathrm{R}} \langle V_{\mathrm{free}} \rangle_0 \tag{4}$$

Here $\langle V_{\mathrm{free}} \rangle_0$ is the free volume available for component 2 in the system and ρ_2^{R} the number density of rods in the reservoir. Eqn. (4) is exactly valid in the limit that $\rho_2^{\mathrm{R}} \to 0$, but higher order terms will play a role for finite ρ_2^{R}. Nevertheless we will use eqn. (4) as an approximation for N_2 for all densities ρ_2^{R}. Substituting eqn. (4) in eqn. (3) and using the Gibbs–Duhem relation,

$$\mathrm{d}\Pi^{\mathrm{R}} = \rho_2^{\mathrm{R}} \, \mathrm{d}\mu_2^{\mathrm{R}} \tag{5}$$

we obtain

$$\Omega = F - \Pi^{\mathrm{R}} f V \tag{6}$$

where Π^{R} is the osmotic pressure of the rods in the reservoir and

$$f = \frac{\langle V_{\mathrm{free}} \rangle_0}{V}$$

is the free volume fraction. As a model for the rods we take spherocylinders (consisting of cylinders with length L and diameter D and capped with two hemi-spheres). For the osmotic pressure Π^{R} of the spherocylinders in the reservoir we use the scaled particle expression,[31–33]

$$\frac{\Pi^{\mathrm{R}} v_2}{k_{\mathrm{B}} T} = \frac{\phi_2^{\mathrm{R}}}{1 - \phi_2^{\mathrm{R}}} + C_2 \left(\frac{\phi_2^{\mathrm{R}}}{1 - \phi_2^{\mathrm{R}}} \right)^2 + C_3 \left(\frac{\phi_2^{\mathrm{R}}}{1 - \phi_2^{\mathrm{R}}} \right)^3 \tag{7}$$

An expression for f can be obtained realizing that according to Widom's particle insertion method[34]

$$\mu^{\mathrm{ex}} = -k_{\mathrm{B}} T \ln f \tag{8}$$

where μ^{ex} is the excess chemical potential of a test hard rod in a sea of hard spheres. Using the scaled particle expression for the excess chemical potential for rods with a volume fraction approaching zero in a sea of spheres[33,35] one obtains

$$f = (1 - \phi_1) \exp\left\{ -\left[A \left(\frac{\phi_1}{1 - \phi_1} \right) + B \left(\frac{\phi_1}{1 - \phi_1} \right)^2 + C \left(\frac{\phi_1}{1 - \phi_1} \right)^3 \right] \right\} \tag{9}$$

Here $\phi_1 = (N_1/V)[(\pi/6)\sigma^3]$ is the volume fraction of the large spheres and the coefficients A, B and C take the form,

$$\begin{aligned} A &= 3q + 3q^2 + q^3 + 1.5r + 3qr + 1.5q^2 r \\ B &= 4.5q^2 + 3q^3 + 4.5qr + 4.5q^2 r \\ C &= 3q^3 + 4.5q^2 r \end{aligned} \tag{10}$$

with $r = L/\sigma$ and $q = D/\sigma$.

From eqn. (6) we obtain using standard thermodynamical relationships,

$$\mu_1 = \left(\frac{\partial \Omega}{\partial N_1} \right)_{\mu_2, V, T} = \mu_1^0 - \Pi^{\mathrm{R}} \frac{\mathrm{d}f}{\mathrm{d}N_1} V \tag{11}$$

$$P = -\left(\frac{\partial \Omega}{\partial V} \right)_{\mu_2, N_1, T} = P^0 + \Pi^{\mathrm{R}} \left(f - V \frac{\mathrm{d}f}{\mathrm{d}V} \right) \tag{12}$$

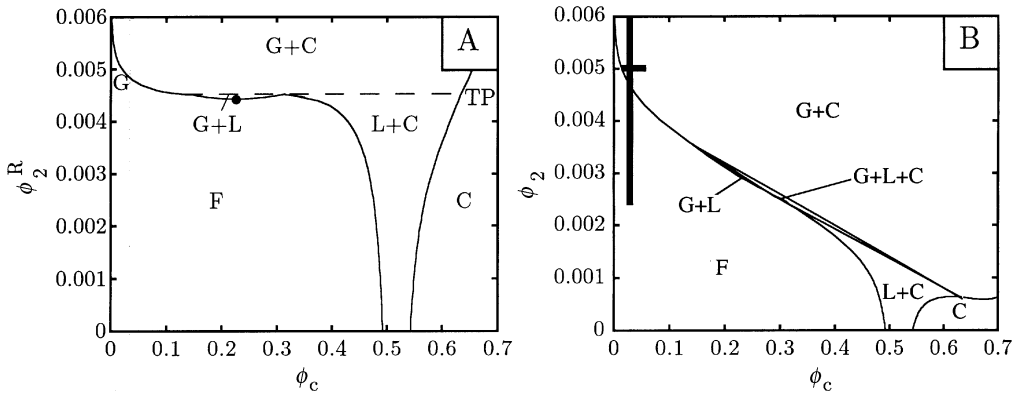

Fig. 2 Phase diagram of the mixture of colloidal spheres and hard colloidal rods. A: On the vertical axis the volume fraction of the rods in the reservoir is plotted *versus* the volume fraction of colloids on the horizontal axis. B: On the vertical axis the volume fraction of the rods in the system is plotted *versus* the volume fraction of colloids on the horizontal axis. The vertical bar at $\phi_c = 0.025$ indicates the window of the experiment.

The phase diagram is obtained by solving the coexistence conditions,

$$\mu_1' = \mu_1'' \tag{13}$$

$$P' = P'' \tag{14}$$

Using the well known expressions for the pressure and chemical potential for the hard sphere fluid (Carnahan and Starling[36]), the hard sphere solid (free volume theory) as well as a reference point for the chemical potential of the hard sphere solid,[37] we are capable of calculating the phase diagrams.

In Fig. 2 we give the phase diagram for $L = 230$, $D = 10$ and $2R = 740$, which happens to be the dimensions of the particles in our experiments. In Fig. 2(A) the large sphere volume fraction in the system is plotted *versus* the volume fraction of rods in the reservoir. In Fig. 2(B) the same phase diagram is given but now the volume fraction of spheres in the system is plotted *versus* the volume fraction of rods in the system. The conversion of the volume fraction in the reservoir ϕ_2^R to the volume fraction rods in the system ϕ_2 is carried out using eqn. (4) leading to,

$$\phi_2 = \phi_2^R f \tag{15}$$

III Experimental

We have prepared mixtures of fluorescent colloidal silica spheres and silica coated boehmite rods dispersed in a solution of 0.001 M LiCl in dimethylformamide (DMF).

The fluorescein isothiocyanate (FITC) labeled silica particles of 370 ± 8 nm radius (dynamic light scattering) were synthesized following van Blaaderen and Vrij.[38] Their fluorescent core is about 372 nm in diameter. Details on synthesis and characterization of the spheres can be found in ref. 39. The spheres form stable suspensions which sediment in a matter of hours, forming a crystalline sediment at the bottom of the vessel. The FITC labeling of the spheres, together with the large size, allow for direct observation of the spheres by confocal microscopy.[30]

The boehmite (γ-AlOOH) rods of length $L = 230 \pm 90$ nm and diameter $D = 9 \pm 2$ nm were synthesized according to the method of Buining *et al.*[40] and coated with a thin layer of silica following the method detailed in refs. 41–43. The silica coating of the rods is applied to make the rods compatible with the silica spheres. The boehmite rods, concentrated to a volume fraction of 0.7%, form a highly viscous suspension.

Mixtures were prepared by weighing in the appropriate amounts of the stock solutions of rods and spheres and adjusting the salt concentration to 0.001 M with LiCl in DMF. The addition of

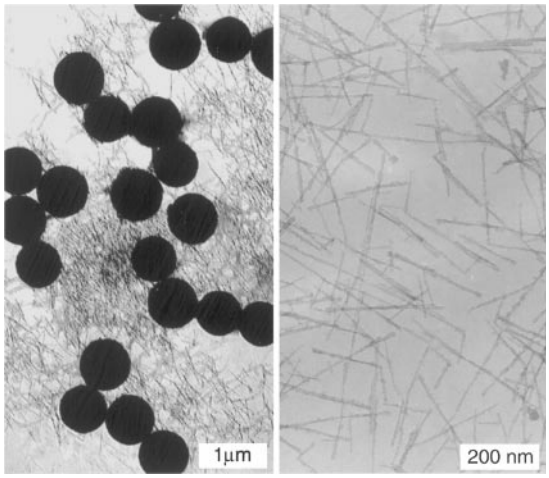

Fig. 3 A: Transmission electron micrograph of a mixture of silica spheres and silica coated boehmite rods. B: Electron micrograph of the rods. Reprinted with permission from *Langmuir*, 1999. ©, 1999 American Chemical Society.

LiCl results in a Debye length $\kappa^{-1} = 9$ nm. The silica rods and spheres disperse without aggregation upon mixing in DMF. Sedimentation measurements[44] on the dilute rod–sphere mixtures were highly reproducible, confirming that the mixtures are indeed stable. In Fig. 3 electron micrographs of our system are given.

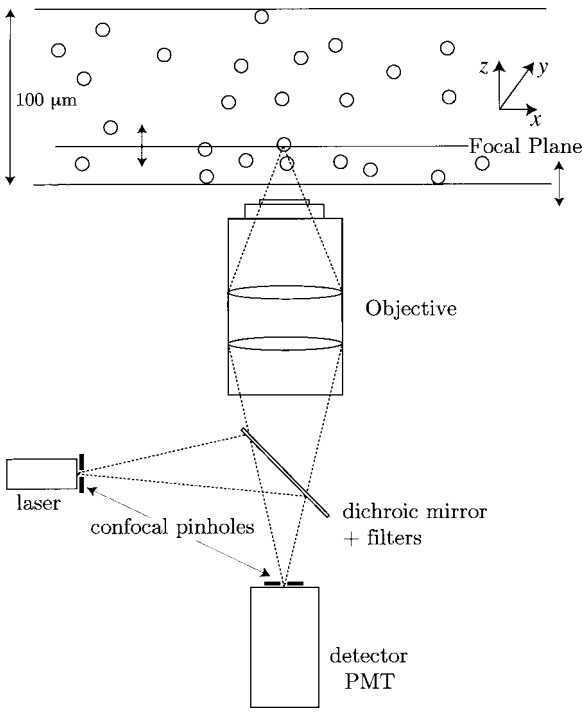

Fig. 4 Setup of experiment. The glass capillary, rectangular 40 mm × 2 mm × 100 μm is positioned horizontally. The lens is at the bottom side of the cuvette (inverted microscope). The sample is beam-scanned in the x–y plane and stage-scanned in the z-direction.

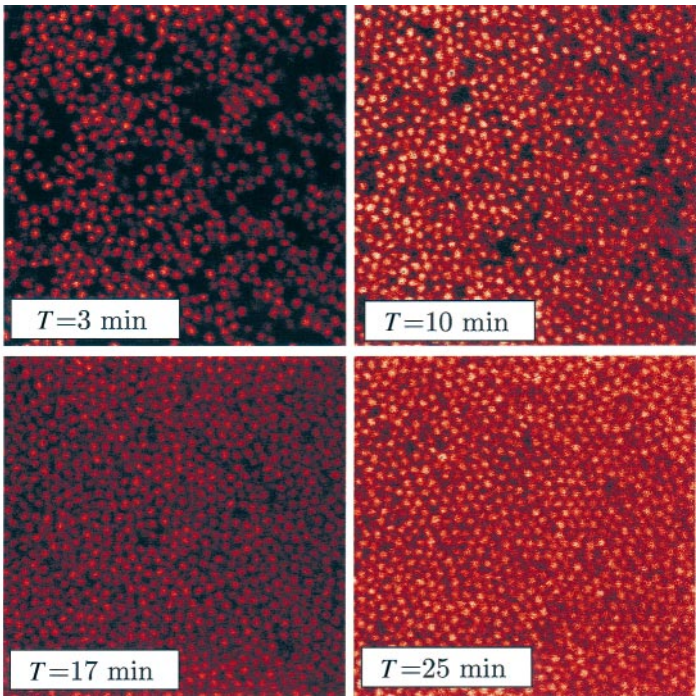

Fig. 5 Time series of a sample of 0.25% rods and 2.5% spheres at the glass wall. In time the density increases without signs of enhanced clustering. The image sizes are 50 × 50 μm.

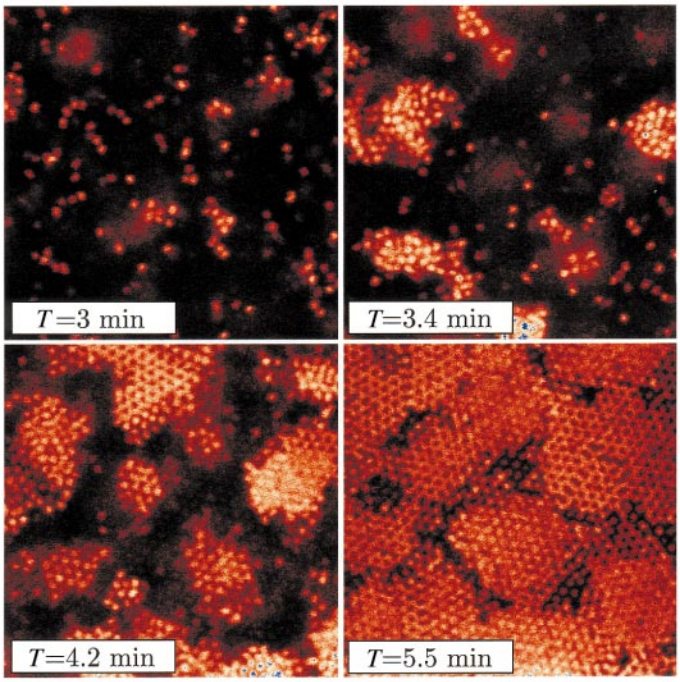

Fig. 6 Time series of a sample crystallizing 10 μm deep in the sample. The rod concentration was 0.5% and the sphere concentration was 2.5%. The first image was taken 3 min after preparation. The image sizes are 50 × 50 μm.

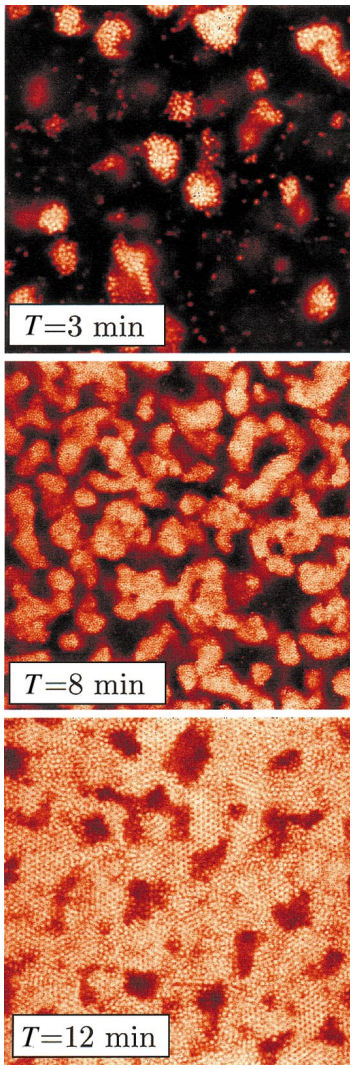

Fig. 7 A: Aggregates as formed initially (3 min) in a sample of a rod volume fraction of 0.5% and a sphere volume fraction of 4.5% at 15 μm in the sample, image size: 50 × 50 μm. **B**: The same system 8 min after preparation. The aggregates cluster to form a bicontinuous network, image size: 100 × 100 μm. C: Image of a late stage (12 min after preparation) "spinodal"-type of network at 0.5% rods and 4.5% spheres. Note that we have here only partial crystalline order, while the large holes are still present, image size: 50 × 50 μm.

Measurements with the confocal microscope were carried out in the following way. Prior to measurements, the particular sample to be studied was carefully mixed on a vortex and a 2 mm wide and 100 μm thick capillary (Vitrodynamics) was filled and sealed. Three min after filling the cuvette, samples were studied under the confocal microscope (Leica TCS NT, equipped with a krypton–argon laser, 1.4 numerical aperture 100 × objective) and 2D and 3D datasets were taken. The time required to take an image of 512 × 512 pixels (voxels) is only 0.25 s, which was sufficiently short for our experiments. In Fig. 4 the setup of the experiment is drawn schematically. In this type of microscope, the capillary is placed in a horizontal orientation. The objective is positioned on the bottom side of the cuvette. Scans were made in time, at the wall and in the bulk and through the sample in the z-direction (vertical) when the system had reached (quasi) equilibrium.

IV Results

We have done experiments in a small window in the phase diagram for which the sphere volume fraction was kept between 1 and 5%, the rod volume fraction was varied between 0.25 and 0.6%.

In Fig. 5 the evolution of a system of 0.25% rods and 2.5% spheres is shown. In this system no signs of depletion induced phase transitions are found. The spheres sediment quite rapidly to the lower glass wall of the capillary, forming a dense fluid phase. In the pictures it is seen that with time the density increases (by sedimentation). Locally ordered structures are formed and broken up again. The process here covers about 25 min.

Fig. 6 shows images of a system of 0.5% rods and 2.5% spheres. In this case the morphology is totally different of that of the system with 0.25% rods. Clusters are rapidly formed (within minutes) and those aggregates rapidly transform into crystallites while they grow and coalesce. The initial clusters contain typically 1000 particles. In the final stage, reorientation of different crystalline patches and annealing of defect lines is seen. This finally results in a large crystalline area. The whole process does not take more than 8 min in this case, which is much faster than in the case of 0.25% rods. This strongly suggests the presence of attractive interactions between the spheres due to the rods.

As the concentration of rods is further increased to 0.6%, the system gets stuck into a gel state in an early stage. Only small aggregates have then been formed (10–25 particles) which cannot grow further. We think this is due to (reversible) gelling of the rods. At the wall, however, small crystallites are still formed.

Increasing the sphere concentration at constant rod concentration (0.5%) leads to a more rapid initial clustering process. However, the subsequent transformation seems to be not as successful as in the case of the lower concentration of spheres. In Fig. 7(A), a typical picture is shown of the initial stage (3 min after preparation) of clusters formed in a mixture of 4.5% spheres and 0.5% rods. The clusters are mostly amorphous and have rounded shapes. Fig. 7(**B**) (8 min after preparation) shows a picture of the subsequent stage of coalescence of clusters, which results in a "spinodal"-type structure. We have to stress however, that these structures have nothing to do with the process of spinodal decomposition. The images show that there is already a partial transformation of amorphous aggregates into crystalline structures. Fig. 7(C) shows a "spinodal"-like structure in this same system (12 min after preparation) of 0.5% rods and 4.5% spheres. Compared to the final structure from Fig. 6 we see here only partial crystalline order while the holes in the structure stay present.

V Discussion and conclusions

Phase separation in rod–sphere mixtures can occur at very low concentrations of rods. In the system studied here the phase transition for sphere volume fractions in the range of 1–5% occurs for rod volume fractions around 0.3%. This is in semi-quantitative agreement with the theoretical calculation. We note that the calculation refers to real hard spheres and real hard rods. Although we think that our spheres approximate hard sphere behavior fairly closely, the rods do show signs of attractive interactions resulting in a slow gelation. This means that our depletion interaction will not be constant in time. However the aggregation and crystallization phenomena take place on a much shorter time-scale (minutes) than the gelation of the rods (hours to days).

The crystallization process was studied on the particle level with confocal scanning laser microscopy. These experiments revealed that the crystallization proceeds *via* a two step pathway. The first step being the rapid formation of aggregates, which subsequently coalesce and transform into crystallites. It appears as if the formation of aggregates as well as the transformation into crystals proceeds without experiencing any barrier. The coalescence of the clusters initially formed leads to an intermediate "spinodal-like" structure. However, this structure is not formed through the mechanism of spinodal decomposition as we observed by direct visual inspection on the particle level.

The two step process observed here is comparable to the aggregation and crystallization phenomena reported in computer simulations[45] and experiments[46] on hard sphere mixtures. A striking

similarity was found between our confocal images and snapshots of particle configurations from recent Brownian dynamics simulations on colloid–polymer mixtures by Soga *et al.*[47]

Finally we note that in addition to the "standard" phase behavior (gas–liquid, gas–solid and fluid–solid equilibria) of colloid–polymer mixtures, and binary mixtures of spherical colloids, rod–sphere mixtures have the additional possibility of orientational ordering of the rods. This type of phase behavior occurs at higher rod concentrations and was observed by Adams *et al.*[48] who have found various new exotic phases in mixtures of the rod-like fd virus and polyethylene or polystyrene spheres. Their work and the results presented here clearly demonstrate that mixed suspensions of colloidal rods and spheres offer the opportunity to study fascinating phase behavior.

Acknowledgement

This work was supported by the Stichting voor Fundamenteel Onderzoek der Materie (Foundation for Fundamental research on Matter) which is part of the Nederlandse Organisatie voor Wetenschappelijk Onderzoek (Netherlands Organization for the Advancement of Research).

References

1 S. Asakura and F. Oosawa, *J. Chem. Phys.*, 1954, **22**, 1255.
2 A. Vrij, *Pure Appl. Chem.*, 1976, **48**, 471.
3 C. Cowell, R. Lin-In-On and B. Vincent, *J. Chem Soc., Faraday Trans. 1*, 1978, **74**, 337.
4 H. de Hek and A. Vrij, *J. Colloid Interface Sci.*, 1979, **70**, 592.
5 P. R. Sperry, *J. Colloid Interface Sci.*, 1984, **99**, 97.
6 B. Vincent, J. Edwards, S. Emmet and R. Croot, *Colloids Surf.*, 1988, **31**, 267.
7 F. Leal Calderon, J. Bibette and J. Bias, *Europhys. Lett.*, 1993, **23**, 653.
8 S. M. Ilett, A. Orrock, W. C. K. Poon and P. Pusey, *Phys. Rev. E*, 1995, **51**, 1344.
9 A. P. Gast, C. K. Hall and W. B. Russel, *J. Colloid Interface Sci.*, 1983, **96**, 251.
10 H. N. W. Lekkerkerker, W. C. K. Poon, P. N. Pusey, A. Stroobants and P. Warren, *Eurphys. Lett.*, 1992, **20**, 559.
11 E. J. Meijer and D. Frenkel, *Phys. Rev. Lett.*, 1991, **67**, 1110.
12 W. C. K. Poon, A. D. Pine and P. Pusey, *Faraday Discuss.*, 1995, **101**, 65.
13 N. A. M. Verhaegh, D. Ashnagi, H. N. W. Lekkerkerker, M. Gigho and L. Cipelletti, *Physica A*, 1997, **242**, 104.
14 Y. Mao, M. E. Cates and H. N. W. Lekkerkerker, *Physica A*, 1995, **222**, 10.
15 H. N. W. Lekkerkerker and A. Stroobants, *Physica A*, 1993, **195**, 387.
16 W. C. K. Poon and P. B. Warren, *Europhys. Lett.*, 1994, **28**, 513.
17 J. S. van Duijneveldt, A. W. Heinen and H. N. W. Lekkerkerker, *Europhys. Lett.*, 1993, **21**, 369.
18 P. D. Kaplan, J. L. Rouke, A. G. Yodh and D. J. Pine, *Phys. Rev. Lett.*, 1994, **72**, 582.
19 A. Imhof and J. K. G. Dhont, *Phys. Rev. Lett.*, 1995, **75**, 1662.
20 A. D. Dinsmore, A. G. Yodh and D. J. Pine, *Phys. Rev. E*, 1995, **52**, 4045.
21 M. Dijkstra, R. van Roij and R. Evans, *Phys. Rev. Lett.*, 1998, **80**, 3787.
22 M. Dijkstra, R. van Roij and R. Evans, *Phys. Rev. Lett.*, 1998, **81**, 2268.
23 M. Dijkstra, R. van Roij and R. Evans, *Phys. Rev. E*, submitted.
24 S. Asakura and F. Oosawa, *J. Pol. Sci.*, 1958, **32**,183.
25 L. Auvray, *J. Phys.* (*Paris*), 1981, **42**, 79.
26 Y. Mao, M. E. Cates and H. N. W. Lekkerkerker, *J. Chem. Phys.*, 1997, **106**, 3721.
27 K. Yaman, C. Jeppesen and C. M. Marques, *Europhys. Lett.*, 1998, **42**, 221.
28 P. Bolhuis and D. Frenkel, *J. Chem. Phys.*, 1994, **101**, 9869.
29 G. H. Koenderink, G. A. Vliegenthart, S. G. J. M. Kluijtmans, A. van Blaaderen, A. P. Philipse and H. N. W. Lekkerkerker, *Langmuir*, submitted.
30 A. van Blaaderen and P. Wiltzius, *Science*, 1995, **270**, 1177.
31 H. Reiss, H. L. Frisch and J. C. Lebowitz, *J. Chem. Phys.*, 1959, **31**, 369.
32 M. A. Cotter, *Phys. Rev. A.*, 1974, **10**, 625.
33 Y. Rosenfeld, *J. Chem. Phys.*, 1988, **89**, 4272.
34 B. Widom, *J. Chem. Phys.*, 1963, **39**, 2808.
35 P. G. Bolhuis and H. N. W. Lekkerkerker, *Physica A*, 1993, **196**, 375.
36 N. F. Carnahan and K. E. Starling, *J. Chem. Phys.*, 1969, **51**, 635.
37 D. Frenkel and A. Ladd, *J. Chem. Phys.*, 1984, **81**, 3188.
38 A. van Blaaderen and A. Vrij, *Langmuir*, 1992, **8**, 2921.
39 A. Imliof and J. K. G. Dhont, *Phys. Rev. E*, 1995, **52**, 6344.

40 P. A. Buining, C. Patmamanoharan, J. H. B. Jansen and H. N. W. Lekkerkerker, *J. Am. Ceram. Soc.*, 1991, **74**, 1303.
41 A. P. Philipse, *Colloids Surf., A*, 1993, **80**, 203.
42 A. P. Philipse, A. M. Nechifor and C. Patmamanoharan, *Langmuir*, 1994, **10**, 4451.
43 M. P. B. van Bruggen, *Langmuir*, 1998, **14**, 2245.
44 S. G. J. M. Kluijtmans, G. H. Koenderink and A. P. Philipse, to be published.
45 T. Biben, P. Bladon and D. Frenkel, *J. Phys.: Condens. Matter*, 1996, **8**, 10799.
46 E. K. Hobbie, *Phys. Rev. Lett.*, 1998, **81**, 3996.
47 K. G. Soga, J. R. Melrose and R. C. Ball, *J. Chem. Phys.*, 1999, **110**, 2280.
48 M. Adams, Z. Dogic, S. L. Keller and S. Fraden, *Nature* (*London*), 1998, **393**, 349.

Paper 9/01165J